Quaternary Science Reviews 276 (2022) 107295

Contents lists available at ScienceDirect

Quaternary Science Reviews

journal homepage: www.elsevier.com/locate/quascirev

Borehole logging and seismic data from Lake Ohrid (North Macedonia/Albania) as a basis for age-depth modelling over the last one million years

A. Ulfers [a, *], C. Zeeden [a], B. Wagner [b], S. Krastel [c], H. Buness [a], T. Wonik [a]

[a] Leibniz Institute for Applied Geophysics, Stilleweg 2, 30655, Hannover, Germany
[b] Institute of Geology and Mineralogy, University of Cologne, Zuelpicher Str. 49a, 50674, Cologne, Germany
[c] Institute of Geosciences, Christian-Albrechts-Universitaet zu Kiel, Otto-Hahn-Platz 1, 24118, Kiel, Germany

ARTICLE INFO

Article history:
Received 29 May 2021
Received in revised form
13 November 2021
Accepted 22 November 2021
Available online xxx

Handling Editor: A. Voelker

Keywords:
Downhole methods
Time-series analysis
Cyclostratigraphy
Seismic interpretation
Sediment properties

ABSTRACT

Robust age-depth models are essential for developing sophisticated interpretations of the sedimentological history in lake basins. In most cases, such models are created using an integrated geoscientific approach, including biostratigraphy, magnetostratigraphy and radiometric dating. In this study, we present an approach to construct age-depth models based on integrating downhole logging and seismic survey data when there are no samples available for dating. An example of this method is shown using data from Lake Ohrid (North Macedonia/Albania).

First, we interpret seismic data and correlate downhole logging data from three sites - DEEP, Pestani and Cerava - to the LR04 benthic stack. We cross-check the resulting age-depth models using cyclostratigraphic methods, which deliver sedimentation rates that are on the same order of magnitude. The maximum age of the investigated sediments is based on lacustrine seismic marker horizons and is approximately 1 million years at DEEP/Pestani and 0.6 million years at Cerava.

In the second step, we construct an artificial lithological log based on cluster analysis using the physical properties of the sediments and integrate it with the age-depth model. This allows an initial interpretation of the sedimentological history at Cerava and Pestani.

Our methodological approach cannot substitute classical sediment core investigations, but we suggest that this two-step approach be applied to future projects of the International Continental Scientific Drilling Program. It can rapidly provide preliminary results on age and sediment type and is particularly useful when datable material is not available.

1. Introduction

1.1. Aim of the study and state of the art

Many studies have been carried out on sediment cores from marine and terrestrial environments to gain insight into climate dynamics and its forcing factors during various geological periods. For the Quaternary, lakes have proven to be valuable climate archives since sedimentation rates are usually high, which yields good temporal resolution of the proxy data. The uniqueness of lake systems is challenging for individual studies and drilling projects, but the results offer the possibility to precisely determine the influence of local climate variability (Litt and Anselmetti, 2014; Melles et al., 2011; Russell et al., 2016; Stein, 2012; Verschuren et al., 2013; Zolitschka et al., 2013).

A crucial step towards interpreting lacustrine sediment records is the development of robust age-depth models. Currently, age estimates in lake drilling projects are often generated using core-based investigations (e.g., Goldstein et al., 2020; Nowaczyk et al., 2013; Shanahan et al., 2013; Stockhecke et al., 2014). This approach is time consuming and can be successful only if suitable core material is available. In some cases, tuning of geophysical downhole logging data has also been applied (e.g., Baumgarten et al., 2015; Baumgarten and Wonik, 2015). Further development

* Corresponding author.
E-mail addresses: Arne.Ulfers@leibniz-liag.de (A. Ulfers), Christian.Zeeden@leibniz-liag.de (C. Zeeden), wagnerb@uni-koeln.de (B. Wagner), sebastian.krastel@ifg.uni-kiel.de (S. Krastel), Hermann.Buness@leibniz-liag.de (H. Buness), Thomas.Wonik@leibniz-liag.de (T. Wonik).

https://doi.org/10.1016/j.quascirev.2021.107295

of an approach to gain chronological information independent of core material can be advantageous for future drilling projects, especially early in a drilling project, when detailed age models based on core material are not available.

One aim of this study is to evaluate the potential, challenges and limits of age-depth models created by using only geophysical downhole logging and seismic data. An example of this is shown for three drill sites (DEEP, Pestani, Cerava) in Lake Ohrid (North Macedonia/Albania). Age-depth models are created through correlation to a reference record. The reliability of the correlation is supported by seismic horizons; the quality of the age-depth models is evaluated using cyclostratigraphic methods on downhole logging data. A second goal is to integrate an artificial lithological log derived from cluster analysis with the time series. This link between the sediment characteristics and the age-depth models provides the first insights into the sedimentological history at the Pestani and Cerava drill sites, as there are no published records for those two sites. A flowchart summarizing the individual steps of all analyses is in the supplement (Fig. S1).

1.2. Site description and sedimentological characterization

Lake Ohrid is located on the Balkan Peninsula between Albania and North Macedonia. From north to south, it extends ~30 km, and from east to west ~15 km, with a maximum water depth of 293 m in the central basin (Fig. 1, Lindhorst et al., 2015). The highest proportion of water input comes from karst aquifers (~50%); direct precipitation and riverine inflow each account for ~25% (Matzinger et al., 2007; Wagner et al., 2010). The surface water has an electrical conductivity of ~200 μS cm^{-1} (corresponding to a resistivity of ~50 Ωm; Matter et al., 2010). Lake Ohrid is considered Europe's oldest lake, and thus, it is a valuable archive for studies that focus on changes in local (hydro)climate during the last 1.36 Myr (e.g., Francke et al., 2016; Wagner et al., 2014, 2019).

Sedimentation processes vary between the investigated drill sites DEEP, Pestani and Cerava (Fig. 1). Francke et al. (2016) presented a detailed sedimentological description of the upper ~250 m from the DEEP site. The sedimentary record consists of mainly undisturbed, continuous, hemipelagic sediments: These include calcareous silty clays deposited during interglacials, with higher primary production and reduced mixing of bottom waters, and clastic, silty clays deposited during glacials, when low primary production and enhanced mixing persisted. Thin (<5 cm), coarse silt/fine sand mass-movement deposits (MMDs) are interspersed sporadically, and several layers of volcanic ash allow tephrostratigraphic analysis (Francke et al., 2016; Leicher et al., 2016, submitted; Wagner et al., 2019).

A high-resolution, core-based age-depth model for the last 1.36 Myr is available for the DEEP site (Francke et al., 2016; Wagner et al., 2019). This age-depth model is based on the correlation of tephra with radiometrically dated proximal ash layers, tuning of the total organic carbon content to orbital parameters and cross-evaluation

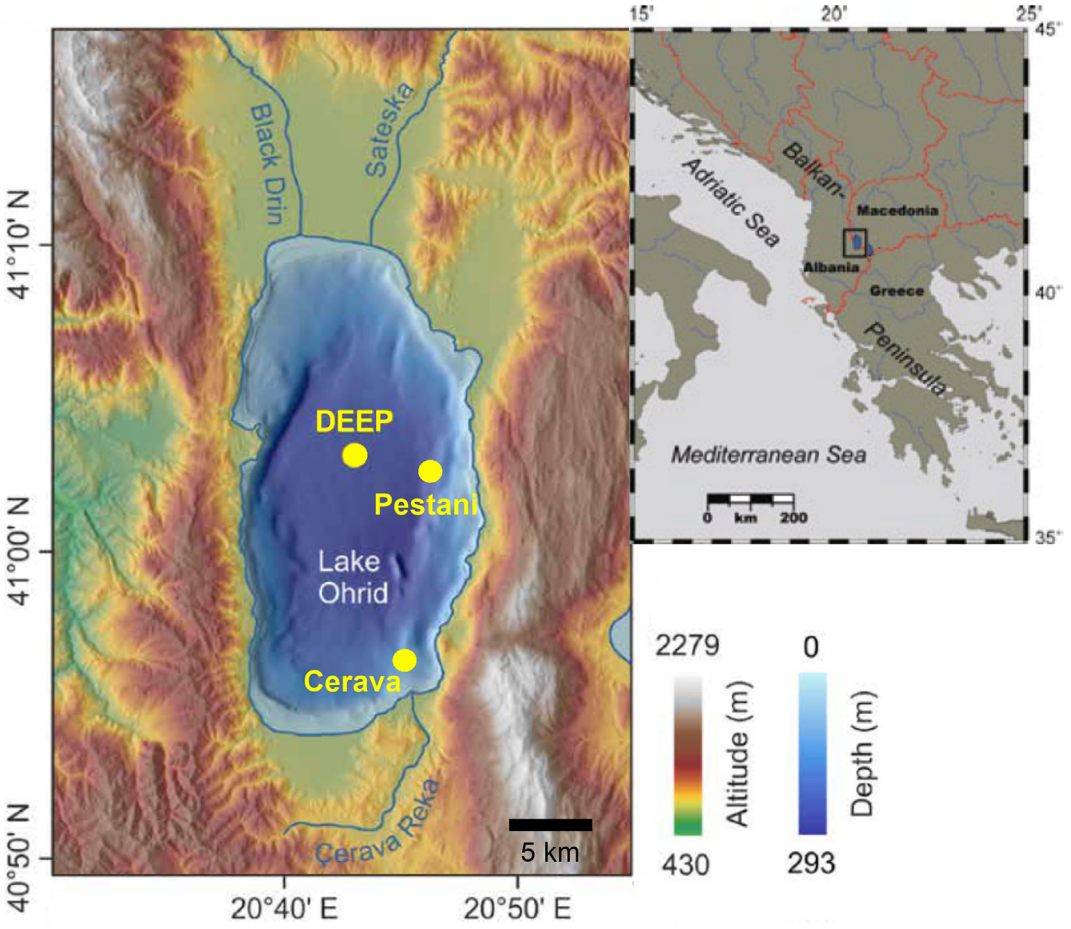

Fig. 1. Digital elevation map and bathymetric overview of Lake Ohrid. Drill sites investigated in this study are marked by yellow circles. Note the position of Cerava in relatively shallow water on the paleodelta close to the southern shore. In comparison, DEEP and Pestani are in the central basin and on its flank, respectively. Modified after Wilke et al. (2020); inset after Lindhorst et al. (2012). (For interpretation of the references to colour in this figure legend, the reader is referred to the Web version of this article.)

of two paleomagnetic age reversals. To date, cyclostratigraphic analysis of downhole logging data has been carried out only on the upper part of the record from the DEEP site, where an age-depth model for the last 630 ka was developed using sliding-window analysis of gamma ray data (Baumgarten et al., 2015).

Age-depth estimates or lithological descriptions of the sediment records from the Pestani and Cerava sites have not yet been published. Seismic interpretations of the Ohrid basin data have focused on the sedimentary and tectonic evolution of the lake (Lindhorst et al. 2010, 2015; Reicherter et al., 2011) and specialized topics such as MMDs (Lindhorst et al., 2012; Wagner et al., 2012b).

2. Material and methods

2.1. Fieldwork

An International Continental Scientific Drilling Program (ICDP) campaign in 2013 was based on several pre-site studies from the early 2000s onwards, which included investigations of short cores (e.g., Matzinger et al., 2007; Vogel et al., 2010a; Wagner et al., 2008) and hydroacoustic surveys (e.g., Lindhorst et al., 2012, 2015; Wagner et al., 2008). During the 2013 drilling campaign, several sites were drilled, some with parallel holes, and composite sediment cores were established. The DEEP site in the central basin (243 m water depth) was selected to obtain an undisturbed and continuous stratigraphic record. The maximum drilling depth was 569 m below the sediment surface, with a core recovery of 95%. The aim at the Pestani site (262 m water depth) was to reach sediments deposited directly above the bedrock at approximately 200 m below the sediment surface. The maximum drilling depth reached 194.5 m with a sediment core recovery of 91%. The Cerava site is located on a lake terrace (125 m water depth) close to the southern shore and was selected to investigate lake level fluctuations that have been indicated by clinoform structures in the subsurface. The maximum drilling depth was 90.5 m below the sediment surface, with a core recovery of 97%. All holes were drilled with a diameter of 149 mm and water-based mud (Baumgarten et al., 2015). Further information about the drilling operations is given in Wagner et al. (2014).

Geophysical downhole logging by the Leibniz Institute for Applied Geophysics acquired continuous datasets of physical properties at the DEEP, Pestani and Cerava sites. The measured parameters were natural gamma radiation (GR), including its components (uranium (U in ppm), potassium (K in %) and thorium (Th in ppm) concentrations), magnetic susceptibility (MS), deep resistivity (R), seismic velocity (Vp), borehole diameter (Cal) and borehole inclination (Dip) (Fig. 2, S2, S3 and S4). As common in unconsolidated (lacustrine) sediments, the GR probe was run inside the drill pipe, while all other probes were run in the open hole after successive lifting of the drill string. We consider the attenuation of the GR signal through the drill pipe as negligible, because it is a systematic error and does not affect the relative change of GR between the different sediment types. The uppermost 30 mblf could not be logged by tools which require open-hole conditions, since drill pipes were kept in the hole to allow downhole probes to enter. This procedure minimizes the risk of a borehole collapse and associated issues such as the inaccessibility of deeper sections or even probe loss. After geophysical downhole logging was completed, all drill pipes were pulled out and the well is abandoned. The vertical resolution of the geophysical downhole logging tools that were used is in the range of ~10–20 cm. A detailed description of logging procedures (e.g., logging speed, diameter of probes, etc.) is given in Baumgarten et al. (2015). General principles of measurements are described by Rider and Kennedy (2011). Data acquisition and (pre)processing were carried out using GeoBase® (Antares, Germany) and WellCAD® (Advanced Logic Technology, Luxembourg).

Multichannel seismic survey data used in our study were recorded with different air gun specifications in 2007 and 2008. In 2007, acquisition gave deeper penetration, whereas in 2008, a higher resolution was preferred (for details see Lindhorst et al., 2015). A total of 47 seismic lines were collected of which we used six in this study (Fig. S5). We used OpendTect© software for seismic interpretation in this study.

2.2. Data processing

The time-depth conversion of seismic profiles was executed with SeisSpace® ProMAX® Seismic Processing Software. The sound velocity of sediments is from average-filtered Vp logs at each site (Figs. S2, S3 and S4), and one average Vp value was calculated every 10 m (Table S1). We used 1480 m/s as the sound velocity of the water body. The time section was shifted until the lake floor reflection coincided with the bathymetric depth after conversion to account for errors in trigger times and/or deviating sound velocities in the water column. The conversion is not valid for complete profiles but restricted to the proximal areas of the drill sites because the complex geologic setting (especially in the lateral parts of the basin) suggests lateral velocity variations. Thus, the correlations between borehole seismic profiles were conducted in the time domain (Figs. S6 and S7).

We traced lacustrine sediment layers from the DEEP to Pestani and Cerava sites. Suitable horizons have to meet two main criteria: They must be continuous between the respective sites, i.e. neither interrupted by faults nor by sedimentary structures like slide deposits. They must be clearly distinguishable from adjacent layers. Tracing was conducted semi-manually using automated tracing (including visual verification) in the central basin and manual picking of sediment horizons in complex settings. In automated tracing, only some points (=seeds) of a horizon are picked and the OpendTect© software follows the horizons to a certain threshold. This technique enables fast tracking, provided that the two criteria described above are fulfilled.

Cyclostratigraphic analyses and sedimentation rate estimates of the upper part (0–240 mblf) of the DEEP site are discussed in Baumgarten et al. (2015). Our cyclostratigraphic investigations were carried out using the 'astrochron' package for the R programming language (Meyers, 2014; R Core Team, 2020). The R code is available in the supplementary material. To evaluate amplitude variations, we used spectral analysis (evolutive harmonic analysis) of (un)tuned records (Thomson, 1982) and wavelet analysis (Gouhier et al., 2019). The latter was conducted using a morlet mother wavelet. Tuned GR data was sampled evenly spaced at 0.5 ka resolution. Other more specific methods include 'testPrecession', an astrochronological testing method, which compares observed precession-scale amplitude modulation to that expected from the theoretical eccentricity solutions. To reduce artificial eccentricity modulations during tuning and data processing, this method implements a series of filters and evaluates the statistical significance of the results using Monte Carlo simulations (Zeeden et al., 2015). The astronomical solution we used is from Laskar et al. (2004). We applied the 'timeOpt', and the 'timeOptTemplate' methods to investigate amplitude modulation and frequency ratios in stratigraphic data and to further determine an optimal time scale for the investigated record. In this study, we utilized linearly decreasing sedimentation rate models with different means and slopes; each of these represents a linearly decreasing sedimentation rate with increasing depth (Meyers et al., 2019).

Cluster analysis was performed using WinSTAT® software for Microsoft Excel®. We created continuous lithological logs for the

physical properties (GR, Th/K, MS, R and Vp). The GR depends on the overall detrital clastics content, while the Th/K ratio is a more specific indicator for different types of clay minerals such as potassium rich feldspar or heavy thorium-bearing minerals (Rider and Kennedy, 2011). MS is determined by the magnetic response (diamagnetic, paramagnetic and ferromagnetic) of the sediment and is mostly used as an indicator for specific mineral compositions. R and Vp are sensitive to porosity and texture of the sediments and give indications on e.g. sorting and grain size (Buecker et al., 2000; Rider and Kennedy, 2011). We used Ward's method as a cluster distance measure (Ward, 1963) and estimated the physical properties for each class in the resulting dendrogram. Subsequently, the classes were colour-coded, imported into Well-CAD® software and compared with core description data (if available).

3. Results

3.1. Logging data

The interval of interest for this study is 0–335 m below lake floor (mblf) at the DEEP site. This interval represents the major part of the lacustrine facies. The lower boundary is given by the interconnection of seismic horizons (Figs. S6 and S7). Although lacustrine sediments occur below this boundary, we refrain from characterizing these parts because the correlation of horizons based on hydro-acoustic data is not unambiguous (see chapter 3.2 Seismic correlation'). The logging data at this site show prominent quasi-cyclicity (Fig. 2), which is particularly visible in the GR and its components (U, K and Th concentrations, as published by Baumgarten et al. (2015) for the upper 240 mblf). The period of the cycles in the GR log decreases below ~260 mblf. MS and R show similar cyclic patterns but are less distinctive above ~170 mblf than below. The upper sections of the MS and R records are characterized by overall increases towards the top. Vp decreases from 38 mblf (top of log) to ~ 110 mblf, where it reaches a minimum of 1330 m/s. Below ~110 mblf, Vp values increase with depth. On average, Vp is 1515 ± 73 m/s in the investigated part of the record. The caliper measurements are relatively constant with some minor peaks and indicate widening of the borehole in the upper part, which is characteristic of boreholes in unconsolidated material. The inclination of <2.5° shows that the drill hole is relatively vertical.

For similar reasons as for DEEP (see above), the interval of interest at Pestani is 0–121.5 mblf, while we investigate the complete record (0–90 mblf) from Cerava. The GR and the U, K and Th concentrations at both sites feature similar cyclic patterns as those at the DEEP site (Figs. S3 and S4). Compared with that of the GR logs, MS and R show similar but less pronounced cyclicity. As at DEEP, increasing values of MS and R occur towards the top in the upper ~70 mblf at Pestani. At Cerava, a sudden increase in R below ~76 mblf coincides with an amplitude change in MS. The sonic velocities at Pestani and Cerava are relatively constant and increase slightly with depth. At both sites, the sonic velocities are low, and Vp averages 1430 ± 20 m/s (min = 1275 m/s; max = 1590 m/s) in the interval of interest at Pestani and 1465 ± 41 m/s (min = 1200 m/s; max = 1730 m/s) at Cerava. The caliper measurements at Pestani indicate that higher GR values correlate with smaller borehole diameters, particularly in the upper ~100 mblf. At Cerava, this correlation is much weaker and present in only the upper 60 mblf. In general, the borehole diameter decreases with depth at both sites. The inclination of both boreholes is commonly less than 5°, defining almost vertical drilling paths.

At all sites, the GR log features the most distinct cyclic patterns compared with other logged parameters. This is why we focus on GR for cyclostratigraphic analysis and time estimates (Chapters 3.3 'Correlation of GR and the LR04 benthic stack' and 3.4 'Cyclostratigraphy'). For the construction of artificial lithological logs, we combine various parameters to make inferences about sediment characteristics (Chapter 3.5 'Cluster analysis'). The integration of age information and sediment characteristics allows an initial description of the sedimentological history at the investigated sites.

3.2. Seismic correlation

Fig. 3 shows depth-converted seismic profiles crossing the investigated sites. While the sediment layers at DEEP are relatively horizontal and well stratified, the geologic situation in the lateral part of the basin is more complex. Disturbed sediments west of Pestani impede tracing of some layers between Pestani and DEEP (Fig. S6). However, certain horizons in the upper and lower parts of the Pestani record can be correlated to DEEP, and age information can be transferred. The dark blue horizon represents the lowermost reliable reflector that connects DEEP and Pestani sites and thus defines the limit of the intervals of interest for this study. Sediments below this horizon are not marked by strong reflectors and interfere with seismic multiples, making a reliable tracing of primary reflectors impossible (Fig. S6).

The correlation of horizons between DEEP and Cerava is hampered by various MMDs in the southern basin (southern part of profile 0820 in Fig. S7). A fault system on the slope of the Cerava plateau adds to the complexity of the setting, and unambiguous tracing of horizons through this zone is impeded (profile 0826 in Fig. S7). Nevertheless, the seismic correlation provides a rough framework for the GR correlation in the lower half of the Cerava record.

Despite not directly affecting the tracing of horizons, several clinoform structures and/or MMDs close to Cerava add complexity to the geology (southern part of profile 0804 in Fig. S7). The main bodies of these structures are located several hundred metres south of the drill site, but their lateral extensions reach the borehole. This interbedding of a different sediment type has a direct influence on the measured parameters in the downhole logs. Depths of all seismic horizons are given in Table S2.

3.3. Correlation of GR and the LR04 benthic stack

To establish a chronology of the Lake Ohrid sedimentation history, the GR logs from the DEEP, Pestani and Cerava sites were correlated with the LR04 stack of Lisiecki and Raymo (2005; Fig. 4). The correlation for the DEEP site follows Baumgarten et al. (2015) and is now extended to ~1 Ma. Most parts of the records from Pestani can also be correlated with the LR04 benthic stack. For Cerava, an unambiguous correlation of the GR record with the LR04 benthic stack is not possible. The more complex geological setting of the Cerava plateau directly influences the cyclic pattern of the GR record. For example, the lateral extension of a clinoform structure at approximately 70 mblf disrupts lacustrine sedimentation and causes a disturbance of the GR signal. At Cerava, information from the seismic correlation is necessary to give an approximate timeframe for our interpretations.

Based on the GR log correlation, the sedimentation rates (SRs) at all three sites were calculated in "cm/ka" for each marine isotope stage (MIS; Fig. 4) using equation (1).

$$SR = \frac{\Delta Depth\ [mblf] * 100}{\Delta Time\ [ka]} \quad \text{(Eq 1)}$$

The mean SR at DEEP is 34.8 cm/ka. The linear trendline of the SR shows an upward increase (dashed blue line in Fig. 4). Moreover, the SR (blue line) in glacial periods is slightly enhanced

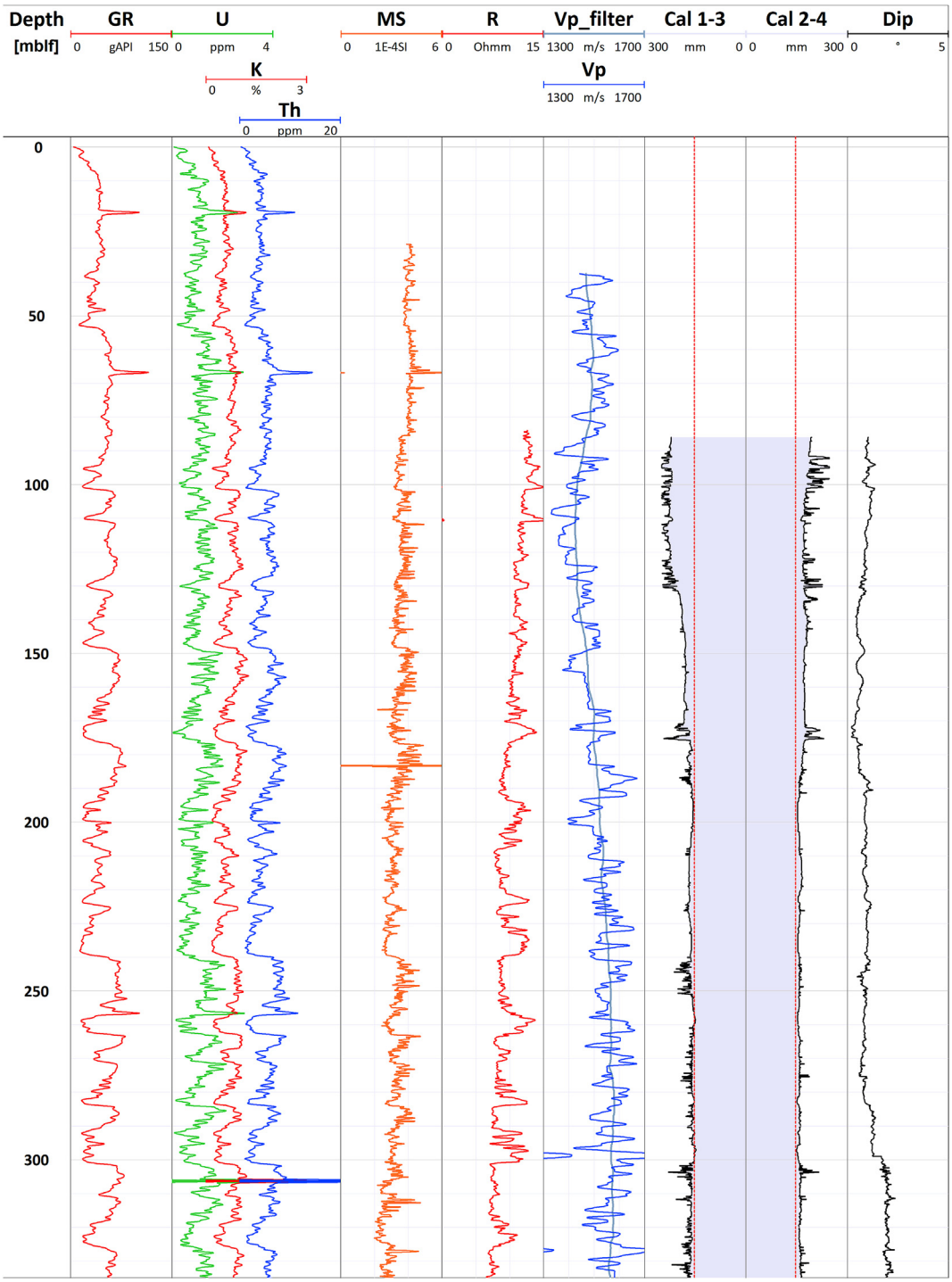

Fig. 2. Section of the downhole logging data from the DEEP site. GR has a distinct cyclic pattern. R increases towards the top in the upper ~170 mblf (probably due to fluid/sediment interaction). Vp increases with depth below ~110 mblf. Abbreviations: mblf = metres below lake floor, GR = natural gamma radiation, U, K and Th concentrations, MS = magnetic susceptibility, R = deep resistivity, Vp = sonic velocity, Vp_filter = sonic velocity filtered with a moving average over 50 m, Cal 1–3, Cal 2–4 = caliper logs/borehole diameter, Dip = dip of drill path, the size of the drill bit is indicated as red dashed line on caliper logs. (For interpretation of the references to colour in this figure legend, the reader is referred to the Web version of this article.)

(mean = 35.5 cm/ka) compared with that in neighbouring interglacial periods (mean = 31.2 cm/ka; e.g., MIS 20, 18, 14 and 06 in Fig. 4).

The SR at Pestani (mean = 13.7 cm/ka) is lower than that at DEEP. The increase in SR towards the upper part of the record is not as pronounced as at DEEP. The SR is slightly increased in interglacials (mean = 14.5 cm/ka) compared with neighbouring glacials (mean = 12.8 cm/ka). MIS 14 exhibits a particularly low SR of 2.7 cm/ka.

The mean SR at Cerava is 15.3 cm/ka. As at DEEP, the SR is

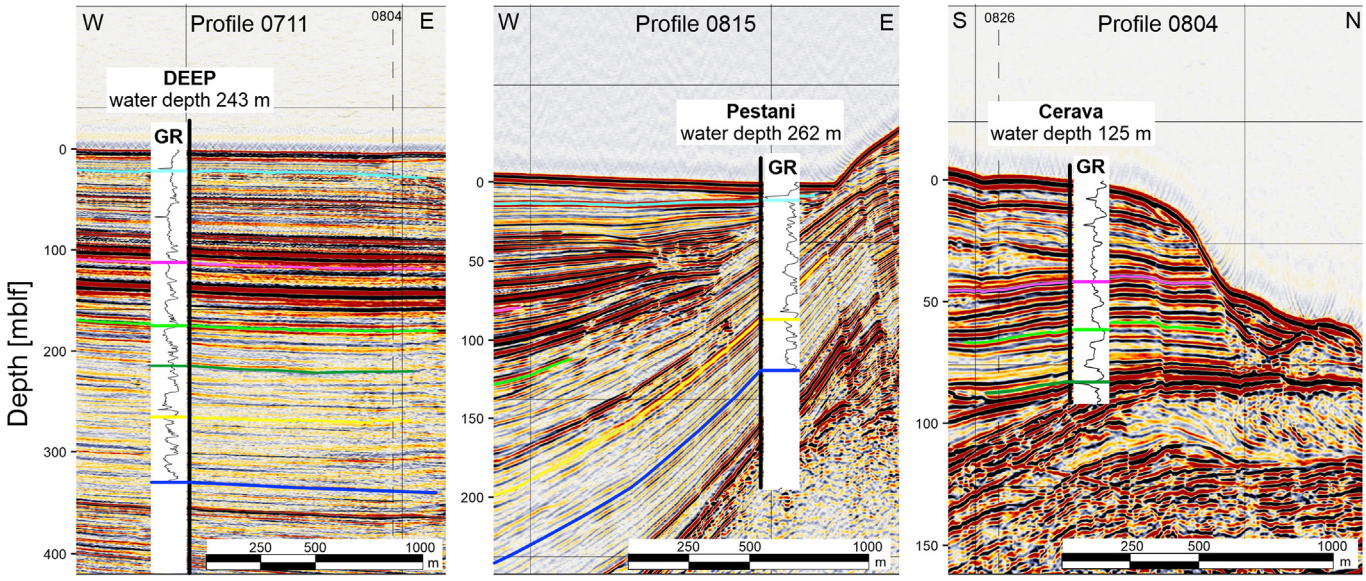

Fig. 3. Seismic profiles at the DEEP, Pestani and Cerava sites after depth conversion. The basis for the correlations between boreholes is shown in Figs. S6 and S7. Schematic natural gamma ray (GR) logs are shown next to each borehole. A detailed plot of GR correlations between all sites, including the coloured seismic horizons, is shown in Fig. 4. Location of seismic lines in an overview map of Lake Ohrid in Fig. S5. Seismic profiles are actually longer, here we show only the vicinity of the respective sites.

enhanced during glacials (mean = 16.0 cm/ka) compared with interglacials (mean = 14.7 cm/ka). Notably, the SR maxima are 32 cm/ka during MIS 6 and 37 cm/ka during MIS 1.

3.4. Cyclostratigraphy

At the DEEP site, the investigated GR record has a length of 335 m (Fig. 5a). As a result of the sliding window approach used for evolutive harmonic analysis, the top and bottom part of a record do not have representative spectra. A similar approach is used in Baumgarten et al. (2015) and the upper 240 mblf are separated into two intervals (45–110 mblf and 110–240 mblf), which are dominated by spectral peaks of 45 m and 30 m wavelengths, respectively. Because cyclostratigraphic features of the upper part are discussed in Baumgarten et al. (2015), we focus on the lower part of the record at DEEP, the corresponding logs obtained at the Pestani and Cerava sites, and additionally apply wavelet analysis.

The dominance of a single frequency in the upper part of the amplitude spectrum at DEEP is replaced by a more complex composition of orbital signals below ~200 mblf (Fig. 5b). Although a strong influence of the 30 m cycle is still present, prominent signals with wavelengths of 75 m and 20 m appear in the record. At depth intervals in which these frequencies attenuate (260-230 mblf and below 280 mblf), high-frequency signals with wavelengths of 13–10 m and 8 m emerge in the record. Wavelet analysis shows a similar shift towards higher frequencies at ~550 ka, where shorter period signals begin to superimpose the long-period signals (Fig. 5c).

The evolutive spectrum for Pestani indicates a similar complexity of dominant cycles with depth (Figs. S8 and S10). A difference from the DEEP site is most evident in a short interval of the upper part (30-20 mblf); various short cycles appear at Pestani, whereas no such configuration of cycles in observable in the upper ~200-45 mblf at DEEP. The limits of the sliding window approach prevent the comparison of the uppermost parts (45-0 mblf at DEEP and 20-0 mblf at Pestani). The main cyclicity throughout the Pestani record has a wavelength between 20 m and 13 m. Other intervals show different spectral properties; especially in the upper (<30 mblf) and the lower depth sections (>90 mblf), where wavelengths of 10 m and 6.5 m occur, respectively.

At Cerava, the clear dominance of any particular spectral peak in the amplitude spectrum is challenging to determine (Figs. S9 and S10). The upper part (55-20 mblf) shows a dominant cyclicity of 12.5 m wavelength, but this peak splits between 30 mblf and 45 mblf. In the lower part (>55 mblf), this dominant signal shifts towards longer periods (17 m), and other cyclicities (9 m and 7 m) appear in the record. As at DEEP, the complexity of cycle components increases with depth, and a single dominant wavelength is not present.

Overall, the GR record at DEEP exhibits a high potential for high-quality cyclostratigraphic investigations, while the patterns from Pestani and especially Cerava are more challenging. At all three sites, the complexity of the orbital signal increases with depth, thus making interpretation more difficult.

We use the timeOptTemplate method (Meyers 2015, 2019) on GR logs from DEEP and Pestani to estimate average SR, utilizing a model with linearly increasing SR (Figs. S11 and S12). Both the average SR and the linearly increasing trendlines of SR towards the top are used to test the depth-age estimates from direct correlation to the LR04 benthic stack (see the mean SR and the quasi-linear trend in Fig. 4, dashed blue lines). The results of both methods and calculated SRs are shown in Table 1.

Using the timeOptTemplate method at DEEP, the best fit for average SR is 35.8 cm/ka (min = 28.7 cm/ka; max = 44.0 cm/ka; Fig. S11), whereas the mean SR derived from direct correlation is 34.8 cm/ka. Comparing the linear trendlines of SR from both methods, the similarity of slopes suggests an almost perfect match of the timeOptTemplate with the LR04 to GR correlation (Fig. S13). The age of sediments at 335 mblf derived through the timeOptTemplate method is estimated to be 935 ka. From Fig. 4, the estimated age at this depth using the direct GR to LR04 correlation is approximately the base of MIS 27 (≙ 982 ka).

At Pestani, the average SR estimates of both methods differ by 2.5 cm/ka: The average SR derived by timeOptTemplate is 16.2 cm/ka (min = 14.4 cm/ka; max = 18.0 cm/ka; Fig. S12), whereas the SR from direct correlation is 13.7 cm/ka. As a result, the age estimate

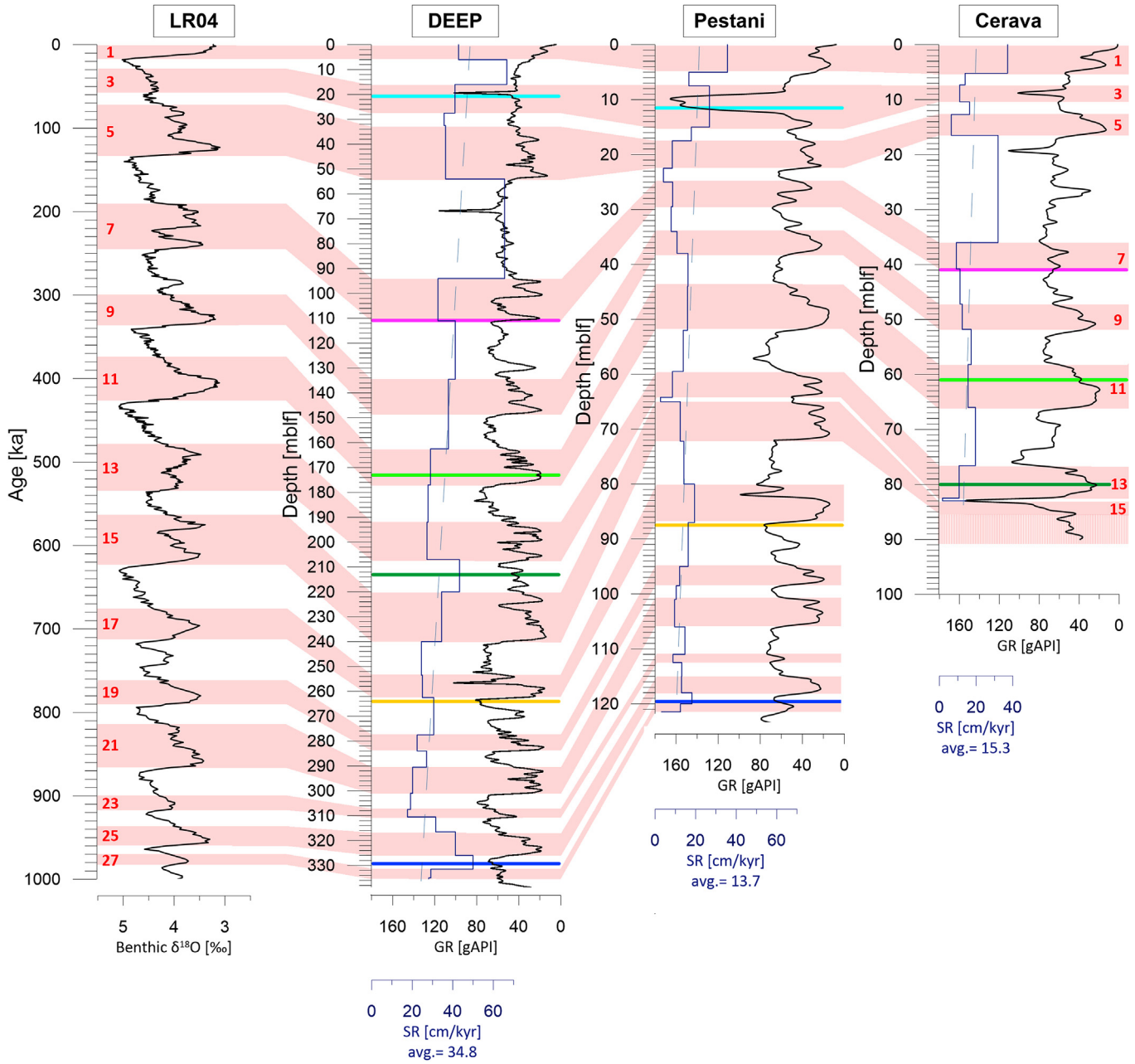

Fig. 4. Correlation of the LR04 benthic stack (Lisiecki and Raymo, 2005) with GR logs from Lake Ohrid. Tiepoints equal the MIS borders. Sedimentation rates (SRs) are plotted in blue. Dashed blue lines are linear trendlines of SRs. Interglacials are indicated in red numbers. Coloured lines are from seismic interpretations (Fig. 3, Table S2). Note that horizons of seismic investigations provide only a rough framework for log-based interpretations. Due to the inaccuracy of time-depth conversion in seismic processing and the different depth scales, they can deviate by several metres from the interpretation of the GR correlation. The interpretation of the upper ~240 mblf at DEEP is similar to the one in Baumgarten et al. (2015). Note the enhanced thickness of marine isotope stage (MIS) 6 at the DEEP and Cerava sites. It is likely that this effect is caused by mass-movement deposits and does not reflect only detrital SRs. Scales for benthic $\delta^{18}O$ and GR are inverted. (For interpretation of the references to colour in this figure legend, the reader is referred to the Web version of this article.)

for a depth of 121.5 mblf is 751 ka for timeOptTemplate but approximately the base of MIS 27 (≙ 982 ka) for direct GR to LR04 correlation. The age is therefore underestimated using the timeOptTemplate approach at the Pestani site. This demonstrates the limitations of this method, as orbital cycles may not be as well preserved at Pestani as they are at DEEP. The generally lower sedimentation rate (with strong minima in e.g. MIS 6 and 14, Fig. 4), and the proximal location of Pestani in the lake basin are two important factors leading to a less accurate recording and preservation of orbital cycles. Since this also applies to Cerava and due to the even shorter record, we do not apply the TimeOptTemplate to Cerava.

3.5. Cluster analysis

Cluster analysis for DEEP was performed using GR, Th/K, MS, R and Vp data over full depth range (Fig. S14), however, we here refer only to the interval of interest (0–335 mblf; Fig. 6). The division into cluster classes is based on dendrograms (Fig. S15) and resulted in well-distinguishable sediment types. The two classes in the interval

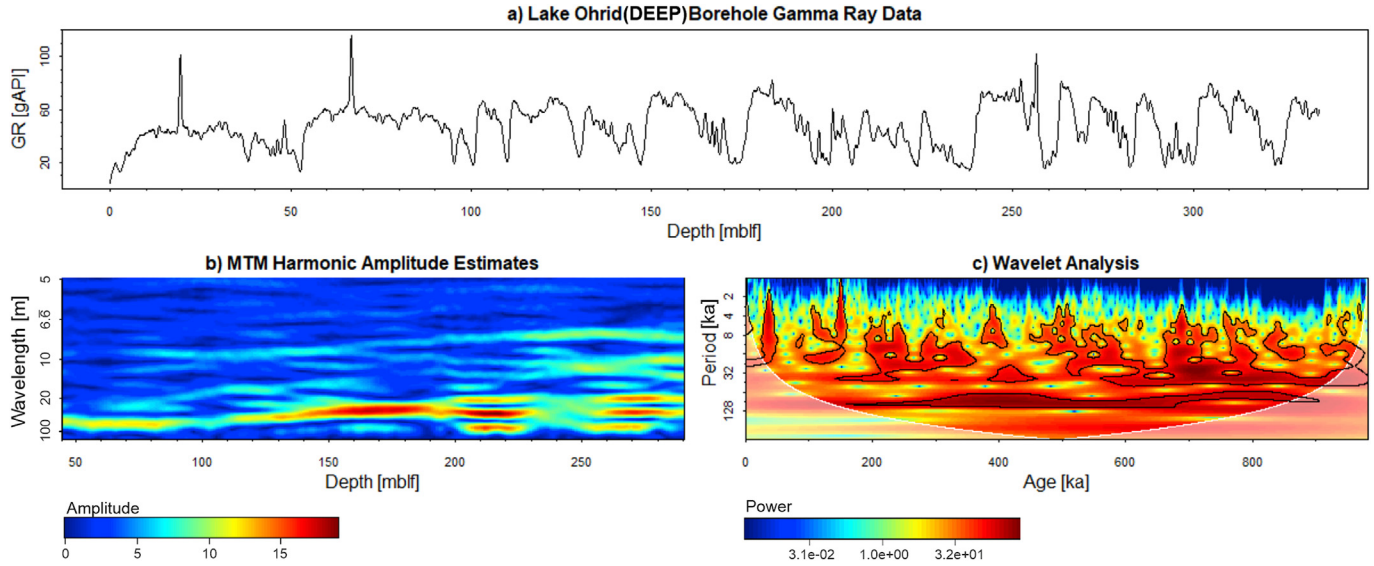

Fig. 5. GR log from the DEEP site (a) and resulting evolutive harmonic analysis (b). Due to window size of 90 m the upper and lower 45 m are missing. Wavelet analysis (c) was performed on the age scale using tie points as shown in Fig. 4.

Table 1
Comparison of two different methods to estimate average sedimentation rates (SRs) and ages at the base of the interval of interest. Values are in cm/ka and ka, respectively.

	DEEP		Pestani	
	SR [cm/ka]	Age at 335 mblf [ka]	SR [cm/ka]	Age at 121.5 mblf [ka]
TimeOptTemplate method	35.8 (28.7–44.0)	935	16.2 (14.4–18.0)	751
Direct GR to LR04 correlation (Fig. 4)	34.8 (17.6–66.7)	982	13.7 (2.7–35.7)	982
Difference in % between both methods	2.8	4.9	16.7	26.7

of interest differ mainly in their GR and R (Fig. 6 and S14). The mismatch between "metres composite depth" (mcd), used in the core descriptions, and "metres below lake floor" (mblf), used in downhole logging, is indicated by grey connections for the interval of interest in Fig. 6. Depth matching for the upper ~250 mblf was performed by Franke et al. (2016) using K counts from XRF core scanning and K concentrations from spectral gamma radiation downhole measurements. We followed the same procedure for the part below 250 mblf. The largest offset of 8.9 m is located in the deeper section (~324 mblf) while almost no shift occurs in the interval of 215–220 mblf (Table S3). These shifts are often caused by expansion effects in the sediment cores, e.g. due to gas release (e.g. Friese et al., 2017; Wagner et al., 2009).

The artificial lithological log and the core description are highly similar. Despite the lower resolution of the artificial log, the correspondence with the core descriptions of Franke et al. (2016) is evident. Strong contrasts in sediment properties are beneficial for grouping sediment types into different classes in a cluster analysis. The "slightly calcareous silty clay" class from the core description depicts a transitional component from calcareous to non-calcareous material and cannot be differentiated in the cluster analysis.

We applied cluster analysis with the same set of parameters and cluster distance measurement methods for Pestani and Cerava (Fig. S14). In both cases, comparison with core material is not possible since the core lithologies are not published.

4. Discussion

4.1. Logging data

Quasi-cyclicity is expressed in all sediment parameters presented in this study and in various proxy data from direct core measurements at the DEEP site (e.g., detrital input, pollen, total inorganic carbon, δ^{18}O-calcite and δ^{13}C-calcite; Wagner et al., 2019). Post-drilling factors, such as fluid intruding the pore space, can bias the downhole logging properties and may weaken or disturb the amplitude of sedimentary proxies related to paleolimnology and paleoclimatology. At DEEP this effect is visible in R above 170 mblf where lake water substitutes/dilutes pore water in the sediment. As the lake water has a relatively higher R of 50–67 Ωm (Wagner et al., 2017) compared to R of the sediment, the average R in the sediment increases. The process of lake water superimposing in situ sediment characteristics is stronger in the upper part, where the longest exposure time to lake water occurred. Similar effects are indicated in the R log at Pestani (Fig. S3). These are challenges to consider in e.g. the interpretation of the cluster analysis.

Another quasi-linear feature at DEEP is the downward increase in Vp below ~110 mblf, which is likely caused by increasing compaction with depth. However, compared with the velocity of typical shale (Erickson and Jarrard, 1998; Rider and Kennedy, 2011), the mean velocity at DEEP is relatively slow (1515 ± 73 m/s), indi-

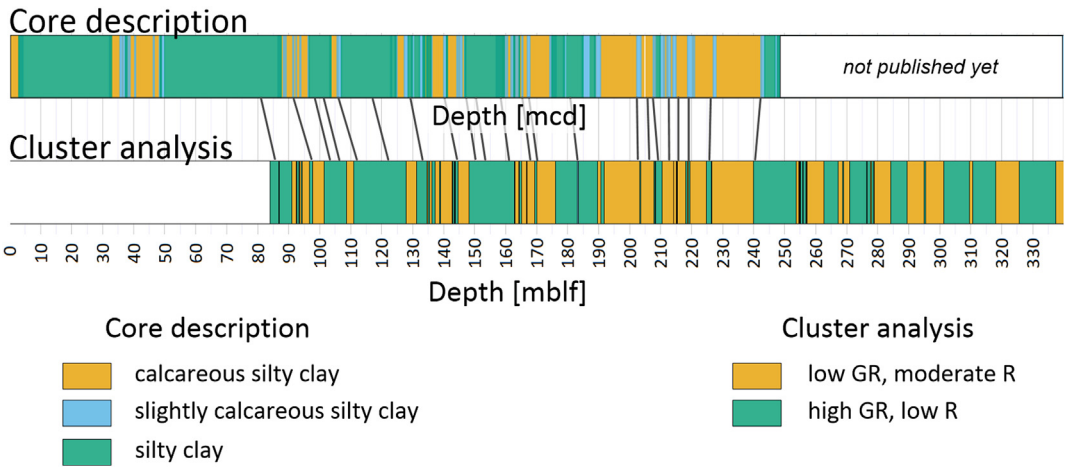

Fig. 6. Comparison of the core description and artificial lithological logs derived from cluster analysis at the DEEP site, showing a high similarity for most parts. Cluster analysis from downhole measurements (in metres below lake floor, mblf) and core descriptions (in metres composite depth, mcd) after Francke et al. (2016) are connected by grey lines indicating depth shifts as listed in Table S3. The legend for cluster analysis is based on values in Fig. S14 and only valid for DEEP down to 335 mblf. Abbreviations: GR = natural gamma radiation, R = deep resistivity. "Slightly calcareous silty clay" is not differentiated in the cluster analysis.

cating highly unconsolidated material. The Vp logs at Pestani and Cerava exhibit similar features (Figs. S3 and S4).

A possible explanation for the minimum of 1330 m/s around 110 mblf at DEEP is a combination of two interrelated factors. Firstly, formation of gas in the pore space. Wagner et al. (2009) describe notable CH_4 release and gas expansion of sediments from piston cores in Lake Ohrid. Secondly, an increase in the caliper of the borehole in this part. The minimum in Vp cannot be accounted to a drastic change in lithology, as the sediments in this area resemble the overall pattern in Lake Ohrid (calcareous silty clay and silty clay; Fig. 6). Low values in Vp are common in (lake) environments with highly unconsolidated material. E.g. in a significant part of the sediments in the upper ~100 m of Lake Towuti (Indonesia), the Vp is below 1400 m/s (Ulfers et al., 2021) and Warrick et al. (1974) describe P-wave velocities of 1360 m/s of unconsolidated mud in the San Francisco Bay.

At the sites other than at DEEP, the caliper logs exhibit a correlation to GR. It implies that sediments with a low GR value can be washed out more easily than sediments with higher GR values. This effect is most important for the low-GR material representing calcareous silty clay deposited during interglacials (Francke et al., 2016). Through the process of outwash, the GR measured in the borehole decreases even further. This "amplification" of the low-GR signature results in a better differentiation of the two main lithologies. This feature intensifies in the upper part of the boreholes.

4.2. Correlative age-depth models

To support the age-depth relationships, we use prominent seismic reflectors deposited during different MISs. Depth shifts between the interpreted seismic horizons and the MIS horizons derived from the GR to LR04 correlation vary by up to several metres (Fig. 4). This is mainly due to the inaccuracy of time-depth conversion in seismic processing and the different depth scales used in seismic investigation and downhole logging. However, the correlation of prominent seismic reflectors at the investigated sites provides a reliable framework for age estimation. Not all identified horizons at the DEEP site are traceable throughout the Ohrid basin. Thinning of sedimentary units beneath the seismic resolution towards the lateral parts of the basin may result in apparent terminations of reflectors. This is relevant for the Pestani site; tectonic features west of the Pestani site further hamper tracing of horizons between Pestani and DEEP (Fig. 3 and S6). The correlation of seismic reflectors from DEEP to Cerava is hindered by tectonically induced slides in the southern central basin (Lindhorst et al., 2012) and by tectonic structures between the southern central basin and the Cerava plateau (Fig. 3 and S7). Despite this being a factor of uncertainty, we suggest using the horizons in Fig. 3 as a framework for the more detailed GR to LR04 correlation (Fig. 4).

In general, the correlation of GR logs from DEEP and Pestani to the LR04 benthic stack is possible, with a few difficulties in the upper part (MIS 1–6). The GR logs from all sites are displayed on a common age scale in Fig. 7. The LR04 benthic stack is very similar to the GR log from DEEP and somewhat less similar to that from Pestani.

Correlating the record from Cerava to both the LR04 benthic stack and the GR logs from the other sites is difficult. In particular, the lower part of the record (older than MIS 11) is complex, and the resulting age-depth model should be considered preliminary.

A comparison of our age-depth model based on geophysical data at DEEP with an independent core-based model from Wagner et al. (2019) shows high similarity between the age models (Fig. 8). We estimate the first age-depth models for the Pestani and Cerava sites using only geophysical downhole logging and seismic data (no sediment core data available). At Pestani, the maximum age of investigation is the base of MIS 27 (≙ 982 ka) at 121.5 mblf. At Cerava, the oldest part of the record is marked by the MIS 14/15 boundary (≙ 563 ka) at 83 mblf. The accurate age of the lowermost part (83–90 mblf) of the record remains unclear at Cerava; thus, the exact position of the MIS 15/16 boundary, if it was recorded as such, is also unclear.

Note that the "metres below lake floor" (mblf) used in this study deviates from the "metres composite depth" (mcd) used in studies using core material (Francke et al., 2016; Wagner et al. 2014, 2019) because the core splicing and sediment expansion after core recovery will naturally result in different composite depths than the borehole logging data (Figs. 6 and 8 and Table S3).

Our data indicate that there are no hiatuses at the DEEP site, which is confirmed by sediment core data (Francke et al., 2016; Wagner et al., 2019). Geophysical downhole logging data are continuous, but detecting small sedimentological hiatuses in the logs may not be possible. Specifically, at Pestani and Cerava site,

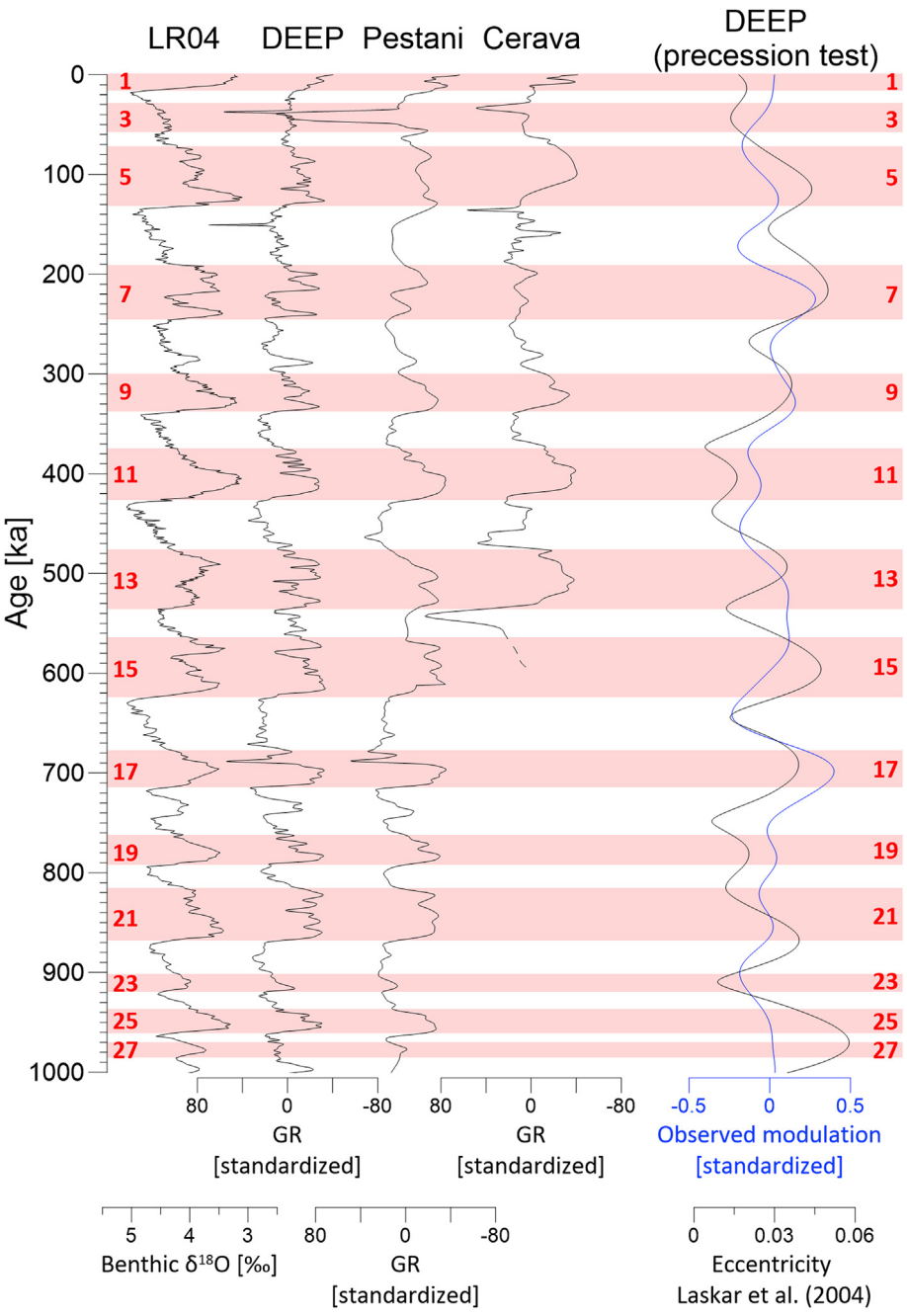

Fig. 7. LR04 benthic stack (Lisiecki and Raymo, 2005) compared to tuned, normalized to mean, GR logs from investigated sites. MIS interglacials are numbered in red. GR is without scale since data were linearly detrended. Whereas the LR04 benthic stack, DEEP GR and Pestani GR correlate relatively well, the sedimentological setting at Cerava complicates the correlation. The dashed line at Cerava during MIS 15 indicates that the record is continuing further down, but we do not assign a definite age to those lowermost ~7 m of Cerava. The precession test for the DEEP site is relevant for the confidence of cyclostratigraphic methods. Blue: observed precession-scale amplitude modulations. Black: theoretical eccentricity from Laskar et al. (2004). See Chapter 4.3 for interpretation. (For interpretation of the references to colour in this figure legend, the reader is referred to the Web version of this article.)

there are stages with lower-than-average SRs (Fig. 4 and Fig. 8), which may include times of no deposition or sediment removal by mass wasting or lake internal currents (Vogel et al., 2010b; Wagner et al., 2012a).

As described by Francke et al. (2016) and Vogel et al. (2010a), SR during glacials is enhanced due to increased hinterland erosion, which is caused by less dense vegetation in the catchment area. We find such trends at DEEP and Cerava, but at Pestani, SR is (on average) higher by 1.7 cm/ka during interglacials. This shows the different sedimentological evolution of the three investigated sites and depicts the local variability of sedimentation history in Lake Ohrid.

4.3. Cyclostratigraphy and time series analysis

The orbital signals in the investigated GR records from Lake Ohrid vary in their characteristics and suitability for statistical cyclostratigraphic analysis. Ideal (lacustrine) records for such studies do not contain hiatuses, have a high depth/temporal resolution, and show the imprint of several orbital cycles. In this study,

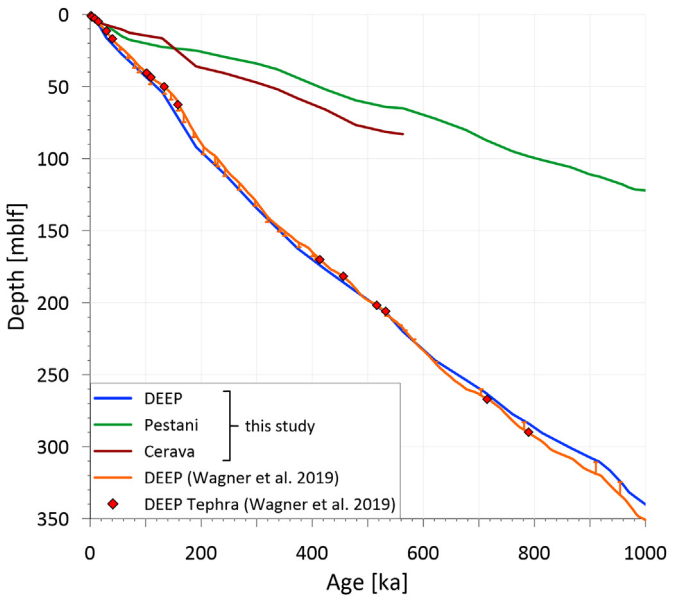

Fig. 8. Age-depth models of investigated sites DEEP, Pestani and Cerava in meters below lake floor (mblf) from geophysical downhole logging. The model from DEEP is compared to data from Wagner et al. (2019). The results from Wagner et al. (2019) are based on the tephrostratigraphic correlation of 16 tephra layers (red diamonds) and tuning of sediment proxy data to orbital parameters. Note that data from Wagner et al. (2019) are in meters composite depth (mcd) based on sediment core measurements. Depth shifts between different depths ("mcd" and "mblf") are indicated as vertical orange bars on data from Wagner et al. (2019) and are based on data in Table S3. We do not show age errors of tephras because error bars are too short to be viewed accurately in this figure (maximum error is ±5.62 ka). Less inclined sections indicate periods of low sedimentation rates and may include hiatuses and/or sediment removal by mass wasting. Steeply inclined sections characterize periods with high sedimentation rates and may include the deposition of mass waste deposits and/or sediments from clinoform structures (Cerava). (For interpretation of the references to colour in this figure legend, the reader is referred to the Web version of this article.)

these criteria hold best for the DEEP site with its setting in the central and deepest part of the lake. At the other sites, which are closer to the shore, tectonic movements and/or mass wasting may bias the orbital signal in the sediments more severely.

Based on the sliding-window approach used by Baumgarten et al. (2015) for the DEEP site, they identify orbital eccentricity and discuss a sharp increase in SR from 30 to 45 cm/ka at 110 mblf. In addition, they use a correlative method involving the LR04 and tephra layers, which is highly similar to our methodological approach. We observe the same change in the amplitude spectrum at 110 mblf (Fig. 5b), but suggest a smooth increase of SR towards the top with a quasi-linear trend (Fig. 4 and S13).

Although SR increases with time towards the recent (Figs. 4 and 8), we initially assume an average SR of ~30 cm/ka for the lower part of the record (200–335 mblf), as this is a precondition for cycle interpretation from the evolutive harmonic analysis (EHA) amplitude spectrum (Fig. 5b and S10). Applying this assumption to interpret the described low-frequency cycles (75 m, 30 m and 20 m wavelengths; see Chapter 3.4 'Cyclostratigraphy') shows that the 30 m period signal represents a combination of the 125 ka- and 95 ka-eccentricity cycle components (Fig. 5b and S10). Following this idea, the prominent signals at 13-10 m and 8 m wavelengths can be identified as obliquity and precession cycles, respectively. A similar shift towards signals with shorter wavelengths is observed in the wavelet analysis (Fig. 5c). This might be related to the decrease in SR and/or indicate a shift to shorter climate cycles towards the deeper part of the record. Our results from the DEEP site are consistent with core-based proxy data (total inorganic carbon and deciduous oak pollen data) from Wagner et al. (2019), which suggest a ~100 ka orbital frequency during the last 700 ka and a pronounced 41 ka orbital frequency before 700 ka. Weak, ~21 ka orbital frequencies occur most prominently in the pollen record (Wagner et al., 2019). This conforms to patterns shown in amplitude spectra (Fig. S10), where prominent eccentricity cycles prevail in the younger part but a more noticeable obliquity component occurs in the older part (>600 ka). We propose that this change is evidence of the Mid-Pleistocene Transition, when a shift from an obliquity-to an eccentricity-dominated world occurs (Pisias and Moore, 1981).

Assuming a constant SR (~14 cm/ka) for the Pestani GR log, the main amplitude (wavelength of 20–13 m; Figs. S8 and S10) represents the 125 ka- and 95 ka-eccentricity cycle. Other prominent cyclicity signals represent obliquity, but precession signals are not detectable in the EHA amplitude spectrum. The wavelet analysis shows a quasi-continuous ~110 ka signal (Fig. S8c), but the obliquity signal vanishes in certain parts, and precession signals cannot be detected. Despite the absence of strong precession cycles, we apply the timeOptTemplate method to estimate SR (Table 1).

The record at Cerava is complex in terms of orbital signal identification. This is probably due to sudden changes in the SR. The EHA data contain a component related to eccentricity and/or glacial/interglacial changes. Obliquity and precession cycles are not obvious, and we therefore refrain from interpreting obliquity and precession cycles at Cerava (Fig. S9).

The reliability of the timeOptTemplate method for estimating SR is based on the quality of precession signals in the investigated records. Testing for precession in the tuned DEEP record was carried out using the method of Zeeden et al. (2015) and is plotted in Fig. 7. The observed match of precession-scale amplitude modulations and the theoretical eccentricity solutions from Laskar et al. (2004) indicate the presence of precession signals for most parts of the GR record. Discrepancies occur in parts at ~520 ka and older than 950 ka, where the precession signal is weak, and the dataset (as in several other late Quaternary datasets; Zeeden et al., 2015) is of limited use for investigating precession amplitude. In the rest of the record, the match of precession amplitude and eccentricity is good for both ~100 ka- and ~400 ka-eccentricity components. It is essential to know that the GR record from the DEEP site has well-resolved precession cycles to use the timeOptTemplate method. In contrast, the SR estimates from timeOptTemplate at Pestani site vary by several cm/ka from the direct GR to LR04 correlation (Table 1). The quality of the precession signal in the GR log from Pestani is also not as obvious as that from DEEP.

The similarity between precession amplitude and eccentricity provides confidence in our age model, especially when considering that the GR record was not tuned to precession but correlated to the LR04 benthic stack only. It is not expected that this leads to artificial similarity. Additionally, the algorithm accounts for correlation-induced signal properties (Zeeden et al. 2015, 2019).

4.4. Integration of cluster lithology in age-depth models

As a final step, we merge information about the timing and sediment characteristics as derived by cluster analysis (Fig. 9). At the DEEP site, sharp contrasts in physical sediment properties allow direct linkage of cluster classes (see Chapter 3.5 'Cluster analysis') to MISs. Difficulties arise when glacial/interglacial changes are not distinctive (e.g., the relatively "warm" glacials MIS 14 and 18 in Fig. 7). and the sedimentation does not completely switch from predominant calcareous silty clay deposition to predominant silty clay deposition or vice versa (e.g., ~215 mblf in Fig. 6 or ~550 ka, which is estimated to be MIS 14, in Fig. 9). This shows that the sedimentation is sensitive to short, suborbital climate change and that sedimentation changes do not strictly occur at MIS boundaries.

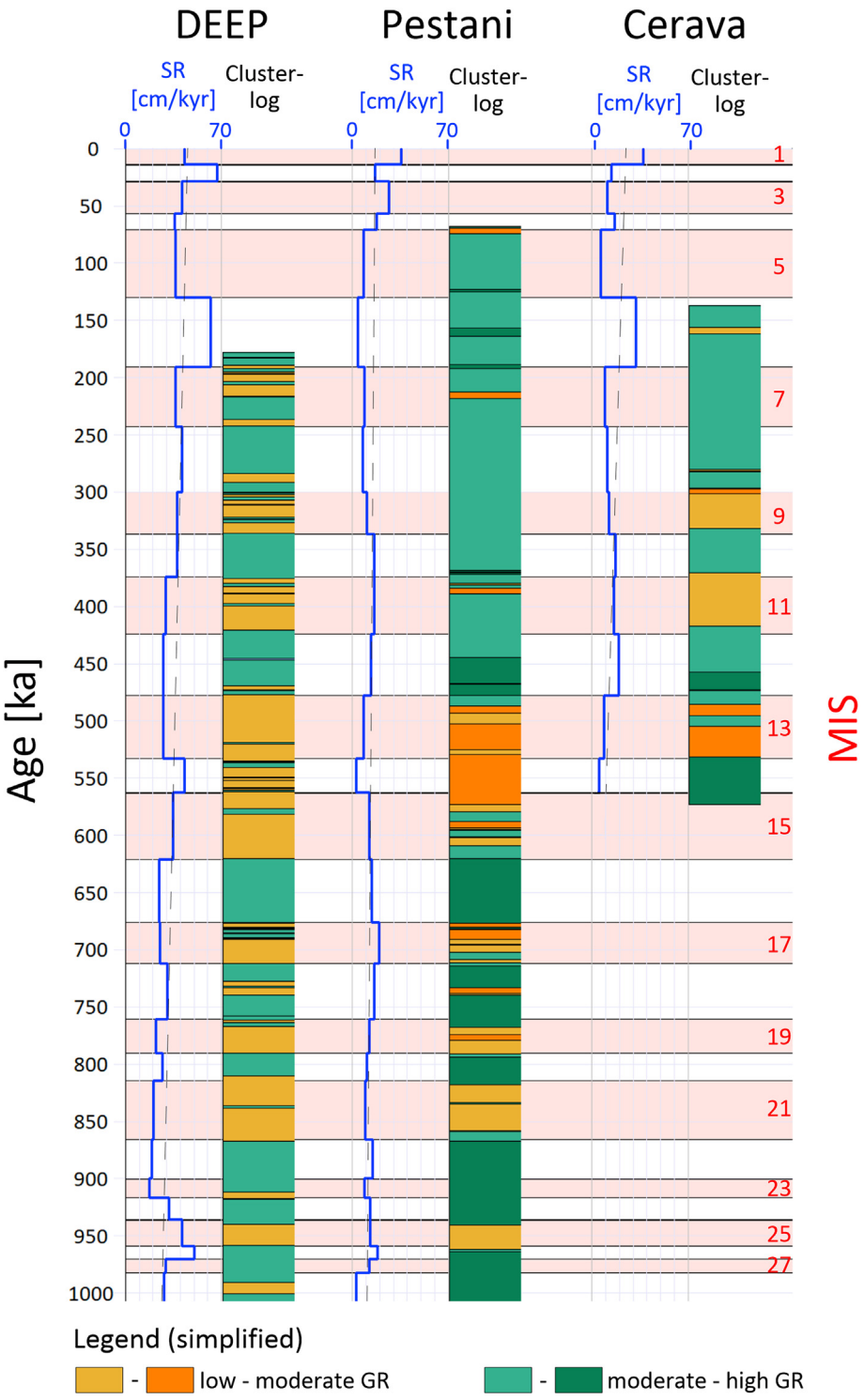

Fig. 9. Artificial lithological log derived by cluster analysis on a time scale. MIS interglacials are indicated in red. Sedimentation rates are in blue as in Fig. 4. Linear sedimentation trends are marked as dashed grey lines. Legend is simplified. Details about the properties of cluster classes are shown in Fig. S14. (For interpretation of the references to colour in this figure legend, the reader is referred to the Web version of this article.)

Despite these effects, physical properties at the DEEP site reflect most MISs for the last ~1 Ma.

Additional information about the characteristics of past environmental changes is provided by the patterns of cluster classes. Sharp contrasts at the bases of interglacials reflect quick changes in the sedimentary system from cold to warm conditions, while changes in cluster classes during the transition from interglacials to glacials document smoother environmental changes (e.g., MIS 19, 17 and 11 of the DEEP record in Fig. 9), as they are known from global climate and ice volume records, including the LR04 benthic stack (e.g., Lisiecki and Raymo, 2005; Imbrie and Imbrie, 1980).

The linkage of cluster lithology to MIS at Pestani is more

challenging. Especially in sediments younger than 450 ka, no clear differentiation of cluster classes exists. In the central part of the Pestani record (960–450 ka), linkage of sediment properties to MISs is possible, although the MIS linkage at Pestani is not as distinct as that at DEEP. At Cerava, the upper part (MIS 6–8) is not differentiated by cluster analysis, but in the older part of the record (>300 ka), the cluster classes are in good agreement with the boundaries of most MISs. In both cases, fluid-sediment interactions may have led to changes in sediment conditions, which superimpose the in situ sediment properties (see increasing R towards the top; Fig. S3). These post-drilling effects could be responsible for the disordered classification of certain segments during the cluster analysis.

4.5. Data quality and uncertainties

Geophysical datasets have to meet certain requirements to provide robust age estimates:

1. Complete/continuous records (MMD or hiatuses are factors adding uncertainty to stratigraphic records).
2. High sedimentation rates (in relation to the vertical resolution of borehole logging tools and seismic data).
3. Distinct changes in climate-sensitive sediment proxies (e.g., high organic matter or $CaCO_3$ accumulation during interglacials and low organic matter and $CaCO_3$ during glacial periods).
4. Preservation of certain orbital parameters in the sediment succession for cyclostratigraphic analysis (e.g., precession signals are essential for the use of the timeOptTemplate method).

The geophysical datasets used in this study meet the listed criteria in different ways. Data from DEEP offer the best quality dataset for the purpose of age estimation. This is demonstrated by the good similarity of the age-depth models from the DEEP site derived in this study by geophysical data and the age-depth model derived for the drilled core by means of a combination of dating methods (Wagner et al., 2019). The criteria are less well met at the Pestani and Cerava sites. Uncertainties emerge at Pestani between MIS 1 and MIS 6, where correlation of the GR log to the LR04 benthic stack is difficult, and at Cerava, where cyclostratigraphic investigations are impeded due to missing precession signals and possible MMDs and/or clinoforms. Nevertheless, distinct changes in climate-relevant sediment proxies and information from seismic reflectors can be traced throughout large parts of the Ohrid basin. This allows for the transfer of age information between individual sites and enables the first reliable age estimations based on geophysical data alone at these sites. Generally, we suggest that our age-depth models are reliable at resolutions greater than glacial/interglacial variability, possibly ~40 ka.

5. Conclusions

This study examines an integrated approach to derive age-depth estimates and lithological descriptions based on geophysical data alone. We use seismic data to trace prominent marker horizons to identify time-equivalent horizons at different drill sites. An age-depth model is established through the correlation of downhole logging data to the LR04 benthic stack (Lisiecki and Raymo, 2005) and by implementation of cyclostratigraphic analysis. We perform cluster analyses on geophysical downhole logging data to generate artificial lithological logs and integrate them into age-depth models.

Sedimentation rates at the three sites, DEEP, Pestani and Cerava, increase towards the tops of the records. During specific glacials or interglacials, opposite patterns of SR at the different sites show that the sedimentation in Lake Ohrid is diverse. This is underlined by seismic data, which show undisturbed sedimentation at DEEP and more disturbed sedimentation at Pestani and Cerava. While sediment properties are able to reflect most of the glacial/interglacial cycles at DEEP, a direct link of sediment properties to MISs is more challenging at Pestani and Cerava sites.

The data for such an investigation have to meet several criteria regarding quality and quantity. An important aspect for cyclostratigraphic analysis is the continuity of the records. Only the DEEP record features no hiatuses or larger MMDs, while sedimentation at Pestani and Cerava is more discontinuous or disturbed. Our study also shows the importance of detailed (seismic) pre-site surveys and a careful selection of drill sites to meet the necessary criteria for robust (cyclostratigraphic) analysis. Various measurements (e.g., geophysical downhole logging and seismic surveys) are required, and multiple statistical methods (e.g., cyclostratigraphy and cluster analysis) must be applied to obtain the first reliable age-depth models and lithological interpretations based on geophysical data alone. This approach has the potential to improve future drilling projects by delivering age-depth models and descriptions of sediment properties before core opening or in cases where no (suitable) core material is available.

Author contributions

Arne Ulfers - Interpretation of the geological/geophysical datasets, performing analyses (cluster analysis/cyclostratigraphy) and writing the major part of the manuscript. Christian Zeeden, - Scientific support and discussion, especially for cyclostratigraphic investigations. Bernd Wagner - Scientific support and discussion, especially for regional geology and sedimentology in Lake Ohrid. Sebastian Krastel - Provision and pre-processing of seismic data. Discussion and support interpreting seismic survey. Hermann Buness - Time-depth conversion of seismic data. Support for chapter 2.2 Data processing. Thomas Wonik - Scientific support and discussion, especially in downhole logging data acquisition and interpretation.

Data availability

The data underlying this article will be shared on reasonable request to the corresponding author.

Declaration of competing interest

The authors declare that they have no known competing financial interests or personal relationships that could have appeared to influence the work reported in this paper.

Acknowledgements

This research project was possible due to funding from the German Research Foundation (grants WO672/10-1 and WO672/15-1/2). The “Scientific Collaboration on Past Speciation Conditions in Lake Ohrid” (SCOPSCO) drilling project was partly funded by grants from the International Continental Scientific Drilling Program (ICDP), the German Ministry of Higher Education and Research, the German Research Foundation, the University of Cologne, the British Geological Survey, the Italian National Institute of Geophysics and Volcanology and the Italian National Research Council and the governments of the republics of North Macedonia (or FYROM) and Albania. We would like to thank the whole SCOPSCO team for helpful discussions about the results. The boreholes were drilled by Drilling, Observation and Sampling of the Earth's Continental Crust, Inc. Our special thanks go to Thomas Grelle, Jan-Thorsten Blanke

and Dr. Henrike Baumgarten of the Leibniz Institute for Applied Geophysics for the acquisition of the geophysical downhole logging data. We also appreciate the work of anonymous reviewers and editors.

Appendix A. Supplementary data

Supplementary data to this article can be found online at https://doi.org/10.1016/j.quascirev.2021.107295.

References

Baumgarten, H., Wonik, T., 2015. Cyclostratigraphic studies of sediments from Lake Van (Turkey) based on their uranium contents obtained from downhole logging and paleoclimatic implications. Int. J. Earth Sci. 104 (6), 1639–1654.

Baumgarten, H., Wonik, T., Tanner, D.C., Francke, A., Wagner, B., Zanchetta, G., Sulpizio, R., Giaccio, B., Nomade, S., 2015. Age-depth model of the past 630 kyr for Lake Ohrid (FYROM/Albania) based on cyclostratigraphic analysis of downhole gamma ray data. Biogeosciences 12, 7453–7465.

Buecker, C.J., Jarrard, R.D., Wonik, T., Brink, J.D., 2000. Analysis of downhole logging data from CRP-2/2A, Victoria Land Basin, Antarctica; a multivariate statistical approach. Terra Antartica 7, 299–310.

Erickson, S.N., Jarrard, R.D., 1998. Velocity-porosity relationships for water-saturated siliciclastic sediments. J. Geophys. Res. Solid Earth 103 (B12), 30385–30406.

Francke, A., Wagner, B., Just, J., Leicher, N., Gromig, R., Baumgarten, H., Vogel, H., Lacey, J.H., Sadori, L., Wonik, T., Leng, M.J., 2016. Sedimentological processes and environmental variability at Lake Ohrid (Macedonia, Albania) between 637 ka and the present. Biogeosciences 13, 1179–1196.

Friese, A., Kallmeyer, J., Axel Kitte, J., Montaño Martínez, I., Bijaksana, S., Wagner, D., 2017. A simple and inexpensive technique for assessing contamination during drilling operations. the ICDP Lake Chalco Drilling Science Team and the ICDP Towuti Drilling Science Team Limnol Oceanogr. Methods 15, 200–211.

Goldstein, S.L., Kiro, Y., Torfstein, A., Kitagawa, H., Tierney, J., Stein, M., 2020. Revised chronology of the ICDP Dead Sea deep drill core relates drier-wetter-drier climate cycles to insolation over the past 220 kyr. Quat. Sci. Rev. 244, 106460.

Gouhier, T.C., Grinsted, A., Simko, V., 2019. R Package Biwavelet: Conduct Univariate and Bivariate Wavelet Analyses, Version 0.20.19.

Imbrie, J., Imbrie, J.Z., 1980. Modeling the climatic response to orbital variations. Science 207 (4434), 943–953.

Laskar, J., Robutel, P., Joutel, F., Gastineau, M., Correia, A.C.M., Levrard, B., 2004. A long-term numerical solution for the insolation quantities of the Earth. Astron. Astrophys. 428 (1), 261–285.

Leicher, N., Zanchetta, G., Sulpizio, R., Giaccio, B., Wagner, B., Nomade, S., Francke, A., Del Carlo, P., 2016. First tephrostratigraphic results of the DEEP site record from Lake Ohrid (Macedonia and Albania). Biogeosciences 13, 2151–2178.

Leicher, N., Giaccio, B., Zanchetta, G., Sulpizio, R., Albert, P., Tomlinson, E., Lagos, M., Francke, A. & Wagner, B., submitted. Lake Ohrid's Tephrochronological Dataset Reveals 1.36 Ma of Mediterranean Explosive Volcanic Activity, Nature Scientific Data.

Lindhorst, K., Vogel, H., Krastel, S., Wagner, B., Hilgers, A., Zander, A., Schwenk, T., Wessels, M., Daut, G., 2010. Stratigraphic analysis of lake level fluctuations in Lake Ohrid: an integration of high resolution hydro-acoustic data and sediment cores. Biogeosciences 11, 3531–3548.

Lindhorst, K., 2012. *Sedimentary and Neotectonic History of Lake Ohrid (Albania/Macedonia): Acquisition and Interpretation of New Hydro-Acoustic and Seismic Data,* PhD Thesis. Christian-Albrechts Universität, Kiel.

Lindhorst, K., Gruen, M., Krastel, S., Schwenk, T., 2012. Hydroacoustic analysis of mass wasting deposits in Lake Ohrid (FYR Macedonia/Albania). In: Yamada, Y., Kawamura, K., Ikehara, K., Ogawa, Y., Urgeles, R., Mosher, D., Chaytor, J., Strasser, M. (Eds.), Submarine Mass Movements and Their Consequences. Advances in Natural and Technological Hazards Research, vol. 31. Springer, Dordrecht, pp. 245–253.

Lindhorst, K., Krastel, S., Reicherter, K., Stipp, M., Wagner, B., Schwenk, T., 2015. Sedimentary and tectonic evolution of lake Ohrid (Macedonia/Albania). Basin Res. 1, 84–101.

Lisiecki, L.E., Raymo, M.E., 2005. A Pliocene-Pleistocene stack of 57 globally distributed benthic δ18O records. Paleoceanography 20 (1).

Litt, T., Anselmetti, F.S., 2014. Lake Van deep drilling project PALEOVAN. Quat. Sci. Rev. 104, 1–7.

Matter, M., Anselmetti, F.S., Jordanoska, B., Wagner, B., Wessels, M., Wuest, A., 2010. Carbonate sedimentation and effects of eutrophication observed at the Kališta subaquatic springs in Lake Ohrid (Macedonia). Biogeosciences 7 (11), 3755–3767.

Matzinger, A., Schmid, M., Veljanoska-Sarafiloska, E., Patceva, S., Guseska, D., Wagner, B., Müller, B., Sturm, M., Wuest, A., 2007. Eutrophication of ancient Lake Ohrid: global warming amplifies detrimental effects of increased nutrient inputs. Limnol. Oceanogr. 52 (1), 338–353.

Melles, M., Brigham-Grette, J., Minyuk, P., Koeberl, C., Andreev, A., Cook, T., Fedorov, G., Gebhardt, C., Haltia-Hovi, E., Kukkonen, M., Nowaczyk, N., Schwamborn, G., Wennrich, V., the Elgygytgyn Scientific Party, 2011. the Lake Elgygytgyn scientific drilling project – conquering Arctic challenges through continental drilling. Sci. Drill. 11, 29–40.

Meyers, S.R., 2014. Astrochron: an R Package for Astrochronology. https://cran.r-project.org/package=astrochron.

Meyers, S.R., 2015. The evaluation of eccentricity-related amplitude modulation and bundling in paleoclimate data: an inverse approach for astrochronologic testing and time scale optimization. Paleoceanography 30 (12), 1625–1640.

Meyers, S.R., 2019. Cyclostratigraphy and the problem of astrochronologic testing. Earth Sci. Rev. 190, 190–223.

Nowaczyk, N.R., Haltia, E.M., Ulbricht, D., Wennrich, V., Sauerbrey, M.A., Rosén, P., Vogel, H., Francke, A., Meyer-Jacob, C., Andreev, A.A., Lozhkin, A.V., 2013. Chronology of Lake El'gygytgyn sediments – a combined magnetostratigraphic, palaeoclimatic and orbital tuning study based on multi-parameter analyses. Clim. Past 9, 2413–2432.

Pisias, N.G., Moore, T.C., 1981. The evolution of Pleistocene climate: a time series approach. Earth Planet Sci. Lett. 52, 450–458.

R Core Team, 2020. R: A Language and Environment for Statistical Computing. R Foundation for Statistical Computing, Vienna, Austria. URL. https://www.R-project.org/.

Reicherter, K., Hoffmann, N., Lindhorst, K., Krastel, S., Fernández-Steeger, T., Grützner, C., Wiatr, T., 2011. Active basins and neotectonics: morphotectonics of the Lake Ohrid Basin (FYROM and Albania) [Aktive Becken und Neotektonik: die Morphotektonik des Ohridbeckens (FYROM und Albanien).]. Zeitschrift der Dtsch. Gesellschaft fuer Geowissenschaften 162 (2), 217–234.

Rider, M., Kennedy, M., 2011. The Geological Interpretation of Well Logs, third ed. Rider-French Consulting Ltd.

Russell, J.M., Bijaksana, S., Vogel, H., Melles, M., Kallmeyer, J., Ariztegui, D., Crowe, S., Fajar, S., Hafidz, A., Haffner, D., Hasberg, A., Ivory, S., Kelly, C., King, J., Kirana, K., Morlock, M., Noren, A., O'Grady, R., Ordonez, L., Stevenson, J., von Rintelen, T., Vuillemin, A., Watkinson, I., Wattrus, N., Wicaksono, S., Wonik, T., Bauer, K., Deino, A., Friese, A., Henny, C., Imran Marwoto, R., Ngkoimani, L.O., Nomosatryo, S., Safiuddin, L.O., Simister, R., Tamuntuan, G., 2016. The Towuti Drilling Project: paleoenvironments, biological evolution, and geomicrobiology of a tropical Pacific lake. Sci. Drill. 21, 29–40.

Shanahan, T.M., Peck, J.A., McKay, N., Heil Jr., C.W., King, J., Forman, S.L., Hoffmann, D.L., Richards, D.A., Overpeck, J.T., Scholz, C., 2013. Age models for long lacustrine sediment records using multiple dating approaches—an example from Lake Bosumtwi, Ghana. Quat. Geochronol. 15, 47–60.

Stein, M., 2012. The ICDP Dead Sea Deep Drilling Project. GSOI.

Stockhecke, M., Kwiecien, O., Vigliotti, L., Anselmetti, F.S., Beer, J., Namik Çağatay, M., Channell, J.E.T., Kipfer, R., Lachner, J., Litt, T., Pickarski, N., Sturm, M., 2014. Chronostratigraphy of the 600,000 year old continental record of Lake Van (Turkey). Quat. Sci. Rev. 104, 8–17.

Thomson, D.J., 1982. Spectrum analysis and harmonic analysis. Proc. IEEE 70 (9), 1055–1096.

Verschuren, D., Olago, D.O., Rucina, S.M., Odhengo, P.O., ICDP DeepCHALLA Consortium, 2013. DeepCHALLA: two glacial cycles of climate and ecosystem dynamics from equatorial East Africa. Sci. Drill. 15, 72–76.

Vogel, H., Wagner, B., Zanchetta, G., Sulpizio, R., Rosén, P., 2010a. A paleoclimate record with tephrochronological age control for the last glacial-interglacial cycle from Lake Ohrid, Albania and Macedonia. J. Paleolimnol. 44 (1), 295–310.

Vogel, H., Wessels, M., Albrecht, C., Stich, H.B., Wagner, B., 2010b. Spatial variability of recent sedimentation in Lake Ohrid (Albania/Macedonia). Biogeosciences 7 (10), 3333–3342.

Wagner, B., Reicherter, K., Daut, G., Wessels, M., Matzinger, A., Schwalb, A., Spirkovski, Z., Sanxhaku, M., 2008. The potential of Lake Ohrid for long-term palaeoenvironmental reconstructions. Palaeogeogr. Palaeoclimatol. Palaeoecol. 259 (2–3), 341–356.

Wagner, B., Lotter, A.F., Nowaczyk, N., Reed, J.M., Schwalb, A., Sulpizio, R., Valsecchi, V., Wessels, M., Zanchetta, G., 2009. A 40,000-year record of environmental change from ancient Lake Ohrid (Albania and Macedonia). J. Paleolimnol. 41, 407–430.

Wagner, B., Vogel, H., Zanchetta, G., Sulpizio, R., 2010. Environmental change within the Balkan region during the past ca. 50 ka recorded in the sediments from lakes Prespa and Ohrid. Biogeosciences 7 (10), 3187–3198.

Wagner, B., Aufgebauer, A., Vogel, H., Zanchetta, G., Sulpizio, R., Damaschke, M., 2012a. Late Pleistocene and Holocene contourite drift in lake Prespa (Albania/FYR of Macedonia/Greece). Quat. Int. 274, 112–121.

Wagner, B., Francke, A., Sulpizio, R., Zanchetta, G., Lindhorst, K., Krastel, S., Vogel, H., Rethemeyer, J., Daut, G., Grazhdani, A., Lushaj, B., Trajanovski, S., 2012b. Possible earthquake trigger for 6th century mass wasting deposit at Lake Ohrid (Macedonia/Albania). Clim. Past 8, 2069–2078.

Wagner, B., Wilke, T., Krastel, S., Zanchetta, G., Sulpizio, R., Reicherter, K., Leng, M.J., Grazhdani, A., Trajanovski, S., Francke, A., Lindhorst, K., Levkov, Z., Cvetkoska, A., Reed, J.M., Zhang, X., Lacey, J.H., Wonik, T., Baumgarten, H., Vogel, H., 2014. The SCOPSCO drilling project recovers more than 1.2 million years of history from Lake Ohrid. Sci. Drill. 17, 19–29.

Wagner, B., Wilke, T., Francke, A., Albrecht, C., Baumgarten, H., Bertini, A., Combourieu-Nebout, N., Cvetkoska, A., D'Addabbo, M., Donders, T.H., Föller, K., Giaccio, B., Grazhdani, A., Hauffe, T., Holtvoeth, J., Joannin, S., Jovanovska, E., Just, J., Kouli, K., Koutsodendris, A., Krastel, S., Lacey, J.H., Leicher, N., Leng, M.J., Levkov, Z., Lindhorst, K., Masi, A., Mercuri, A.M., Nomade, S., Nowaczyk, N., Panagiotopoulos, K., Peyron, O., Reed, J.M., Regattieri, E., Sadori, L., Sagnotti, L., Stelbrink, B., Sulpizio, R., Tofilovska, S., Torri, P., Vogel, H., Wagner, T., Wagner-Cremer, F., Wolff, G.A., Wonik, T., Zanchetta, G., Zhang, X.S., 2017. The

environmental and evolutionary history of Lake Ohrid (FYROM/Albania): interim results from the SCOPSCO deep drilling project. Biogeosciences 14, 2033–2054.

Wagner, B., Vogel, H., Francke, A., Friedrich, T., Donders, T., Lacey, J.H., Leng, M.J., Regattieri, E., Sadori, L., Wilke, T., Zanchetta, G., Albrecht, C., Bertini, A., Combourieu-Nebout, N., Cvetkoska, A., Giaccio, B., Grazhdani, A., Hauffe, T., Holtvoeth, J., Joannin, S., Jovanovska, E., Just, J., Kouli, K., Kousis, I., Koutsodendris, A., Krastel, S., Lagos, M., Leicher, N., Levkov, Z., Lindhorst, K., Masi, A., Melles, M., Mercuri, A.M., Nomade, S., Nowaczyk, N., Panagiotopoulos, K., Peyron, O., Reed, J.M., Sagnotti, L., Sinopoli, G., Stelbrink, B., Sulpizio, R., Timmermann, A., Tofilovska, S., Torri, P., Wagner-Cremer, F., Wonik, T., Zanchetta, G., 2019. Mediterranean winter rainfall in phase with African monsoons during the past 1.36 million years. Nature 573 (7773), 256–260.

Ward Jr., J.H., 1963. Hierarchical grouping to optimize an objective function. J. Am. Stat. Assoc. 58 (301), 236–244.

Wilke, T., Hauffe, T., Jovanovska, E., Cvetkoska, A., Donders, T., Ekschmitt, K., Francke, A., Lacey, J.H., Levkov, Z., Marshall, C.R., Neubauer, T.A., Silvestro, D., Stelbrink, B., Vogel, H., Albrecht, C., Holtvoeth, J., Krastel, S., Leicher, N., Leng, M.J., Lindhorst, K., Masi, A., Ognjanova-Rumenova, N., Panagiotopoulos, K., Reed, J.M., Sadori, L., Tofilovska, S., Van Bocxlaer, B., Wagner-Cremer, F., Wesselingh, F.P., Wolters, V., Zanchetta, G., Zhang, X., Wagner, B., 2020. Deep drilling reveals massive shifts in evolutionary dynamics after formation of ancient ecosystem. Sci. Adv. 6 (40), eabb2943.

Zeeden, C., Meyers, S.R., Lourens, L.J., Hilgen, F.J., 2015. Testing astronomically tuned age models. Paleoceanography 30 (4), 369–383.

Zeeden, C., Meyers, S.R., Hilgen, F.J., Lourens, L.J., Laskar, J., 2019. Time scale evaluation and the quantification of obliquity forcing. Quat. Sci. Rev. 209, 100–113.

Zolitschka, B., Anselmetti, F., Ariztegui, D., Corbella, H., Francus, P., Lücke, A., Maidanah, N.I., Ohlendorf, C., Schäbitz, F., Wastegård, S., 2013. Environment and climate of the last 51,000 years–new insights from the Potrok Aike maar lake Sediment Archive Drilling prOject (PASADO). Quat. Sci. Rev. 71, 1–12.